JMPM: Jurnal Material dan Proses Manufaktur
Vol. 9, No. 1, p36-49, Juni 2025
DOI: https://doi.org/10.18196/jmpm.v9i1.27332

CFD Study on Wire Mesh Inserts Enhancing Heat Transfer in Double Pipe Heat Exchanger

Rizky Nanda Parely[a,1], Nanang Ruhyat[a,2]

[a] Master Program in Mechanical Engineering, Faculty of Engineering, Universitas Mercu Buana, Jl. Raya Meruya Selatan No.1, Kembangan, Jakarta Barat 11650, Indonesia
e-mail: rizkynandaparely2@yahoo.com [1], nanang.ruhyat@mercubuana.ac.id[2]

Correspondence author: rizkynandaparely2@yahoo.com

Keywords:

Double Pipe Heat Exchanger; Wire Mesh, CFD, ANOVA, Heat Transfer.

ABSTRACT

The efficiency of heat transfer in conventional double pipe heat exchangers (DPHE) was often limited by low heat transfer coefficients. This posed a challenge for compact-scale industrial applications requiring enhanced thermal performance without increasing system dimensions. One potential solution was the insertion of wire mesh inside the pipe to induce local turbulence and intensify forced convection. This study was conducted numerically using Computational Fluid Dynamics (CFD) in ANSYS Fluent 2024 R2. The DPHE consisted of concentric copper pipes with a length of 1240 mm, inner pipe diameter of 26/34 mm, and outer pipe diameter of 68/76 mm. Water was used as the working fluid in counterflow mode, with inlet hot water at 70 °C (Re 4000–16000) and cold water at 31 °C (Re 2000). The parameters varied were wire mesh angle (30°, 60°, 90°), wire spacing (3 mm, 4 mm, 5 mm), and mesh spacing (4 cm, 5 cm, 6 cm), arranged using an L9 orthogonal array. Three-way ANOVA and Tukey HSD test were applied to identify significant effects. The configuration of 30°, 3 mm, and 4 cm was found to be the most optimal, yielding a 34.55% increase in heat transfer compared to the plain DPHE.

1. INTRODUCTION

A heat exchanger is a thermal device that functions as either a heater or a cooler, where the heat exchange process occurs due to a temperature difference between two fluids [1]. Several types of heat exchangers exist, one of which is the double pipe heat exchanger (DPHE) [2]. A heat exchanger operates by transferring heat from a high-temperature fluid to a low-temperature fluid [3]. However, heat exchangers are also susceptible to fouling, which refers to the accumulation of unwanted materials on the internal surfaces, and this can significantly reduce thermal performance [4].

In recent years, the application of wire mesh inserts has gained traction in various real-world thermal systems, including automotive radiators, HVAC (Heating, Ventilation, and Air Conditioning) systems, and chemical processing equipment. Their ability to passively enhance heat transfer without increasing the exchanger's footprint has proven advantageous in compact and energy-efficient designs. Additionally, implementations in solar thermal collectors and microelectronics cooling systems further demonstrate the industrial relevance and growing adoption of wire mesh technology in enhancing thermal performance [5][6].

The double pipe heat exchanger is widely applied due to its relatively simple construction, versatility across various industrial processes, low capital investment, and ease of maintenance [7]. In Indonesia, several industries utilize double pipe heat exchangers. For example, PT Kilang Pertamina Internasional applies it for cooling crude oil and supporting fuel processing. Dieng Geothermal Power Plant uses it to condense steam during electricity generation. PT Sawit Sumbermas Sarana employs it in palm oil refining processes, while PT Pabrik Kertas Tjiwi Kimia uses it in pulp bleaching and chemical treatment. Another important application of the double pipe heat exchanger is as an oil cooler, which functions to maintain stable oil temperatures in engines during continuous operation. If oil temperature rises excessively, its

viscosity decreases, thereby reducing its effectiveness as a lubricant. The presence of an oil cooler helps prevent such degradation and ensures consistent system efficiency [8].

Despite its benefits, the double pipe heat exchanger has several limitations. These include restricted heat transfer area due to the narrow pipe geometry, relatively low heat transfer coefficients compared to other exchanger types, and limited suitability for high flow rates or large temperature differences [9]. One approach to overcome these drawbacks is the insertion of wire mesh inside the inner pipe to enhance thermal performance.

Wire mesh plays an important role in improving the effectiveness of double pipe heat exchangers. When inserted into the inner tube, it promotes local turbulence, thereby increasing the convective heat transfer rate between the two working fluids. In addition to thermal enhancement, wire mesh also assists in trapping particles or debris, which can reduce the risk of fouling and internal blockages [10][11]. Thus, a detailed study is needed to evaluate the thermal performance of double pipe heat exchangers equipped with wire mesh inserts.

Key geometric parameters of the wire mesh that influence heat transfer include the inclination angle, spacing between wires, and the spacing between mesh layers. A higher inclination angle tends to intensify convective heat transfer, although it may also increase fluid resistance. Smaller wire spacing and mesh spacing can enhance turbulence and improve heat transfer but may lead to greater frictional losses [11].

Several previous studies have explored the thermal performance of wire mesh inserts using both experimental and numerical methods. Sayed et al. [10] and Kurian et al. [12] conducted experimental investigations on cross-flow heat exchangers, showing significant Nusselt number improvements with various wire mesh spacings. Usama et al. [13] extended this approach numerically, also in cross-flow configurations. In the context of double pipe heat exchangers, Fuskele et al. [11], Gaikwad et al. [14], and Sharifi et al. [15] examined twisted or helical wire mesh inserts, focusing primarily on single-variable designs or specific insert geometries. However, these studies did not comprehensively evaluate the combined influence of mesh inclination angle, wire spacing, and axial spacing within a systematic CFD framework. Moreover, the integration of statistical tools such as three-way ANOVA for evaluating interaction effects remains limited in the current literature. This gap underlines the novelty of the present study, which numerically investigates the simultaneous effects of three geometric parameters using ANSYS Fluent and statistical analysis through IBM SPSS to identify the most thermally efficient wire mesh configuration.

Based on this background, the current study investigates the influence of wire mesh inserts on the thermal performance of a double pipe heat exchanger. The main variables include wire mesh angle, wire spacing, and axial mesh spacing. The simulation focuses solely on the enhancement of heat transfer rate. The results of this study are expected to serve as a scientific reference for the thermal optimization of compact heat exchanger systems in industrial applications.

2. METHODS

This research employs an experimental approach designed to evaluate the effect of specific treatments on the research object. The primary objective is to investigate the influence of wire mesh inclination angle, wire spacing, and axial mesh spacing on the heat transfer rate, aiming to determine the most efficient design for a double pipe heat exchanger. The study utilizes Computational Fluid Dynamics (CFD) as the analytical method. The process begins with geometric modeling using the SpaceClaim feature in ANSYS, followed by numerical simulation using ANSYS Fluent 2024 R2.

2.1 Research Variables

2.1.1 Independent Variables

The independent variables are factors that directly affect the outcome of the research process. In this study, the independent variables include the inclination angle of the wire mesh, the spacing between the wires, and the axial spacing between wire mesh inserts. The detailed configurations of these variables are presented in Table 1.

Table 1. Independent Variables

Wire Mesh Angle			Wire Spacing			Axial Mesh Spacing		
1	2	3	1	2	3	1	2	3
30°	60°	90°	3 mm	4 mm	5 mm	4 cm	5 cm	6 cm

2.1.2 Controlled Variables

Controlled variables are held constant to ensure that the effect of the independent variables on the dependent variables is not influenced by external factors. The controlled variables in this study were:

1) The Reynolds number for cold water was 2000, with an inlet temperature of 31 °C on the outer tube side.
2) The Reynolds number for hot water was 4000–16000, with inlet temperature of 70 °C on the inner tube side.
3) Ambient air temperature was 23 °C.
4) The material for both tubes and wire mesh was copper.

2.1.3 Dependent Variables

Dependent variables are those affected by the changes in independent variables. The dependent variable in this study is the Nusselt number of the double pipe heat exchanger.

2.2 Parameter Input and Selection

An orthogonal array (OA) is used to determine the minimum number of experimental combinations needed to obtain effective results. Each factor in this study consists of three levels: wire mesh angle (A), wire spacing (B), and axial mesh spacing (C), resulting in a total of 27 possible combinations. To reduce computational time without significantly affecting accuracy, the L9 orthogonal array is selected. The OA matrix is presented in Table 2.

Table 2. L9 Orthogonal Array Matrix

Configuration	A (Angle)	B (Wire Spacing)	C (Mesh Spacing)
1	1	1	1
2	1	2	2
3	1	3	3
4	2	1	2
5	2	2	3
6	2	3	1
7	3	1	3
8	3	2	1
9	3	3	2

The symbols A, B, and C correspond to wire mesh angle, wire spacing, and mesh spacing, respectively. Levels 1, 2, and 3 represent the parameter values as shown in Table 1.

2.3 Materials

The research employed a double pipe heat exchanger design as the subject of investigation. Figures 1, 2, and 3 illustrate the geometry of the double pipe heat exchanger used in this study. The plain heat exchanger design was adopted from the study conducted by Kotian et al. [16]. The dimensional specifications of the design are presented as follows:

- Inner pipe inner diameter : 26 mm
- Inner pipe outer diameter : 34 mm
- Outer pipe inner diameter : 68 mm
- Outer pipe outer diameter : 76 mm
- Pipe length : 1240 mm

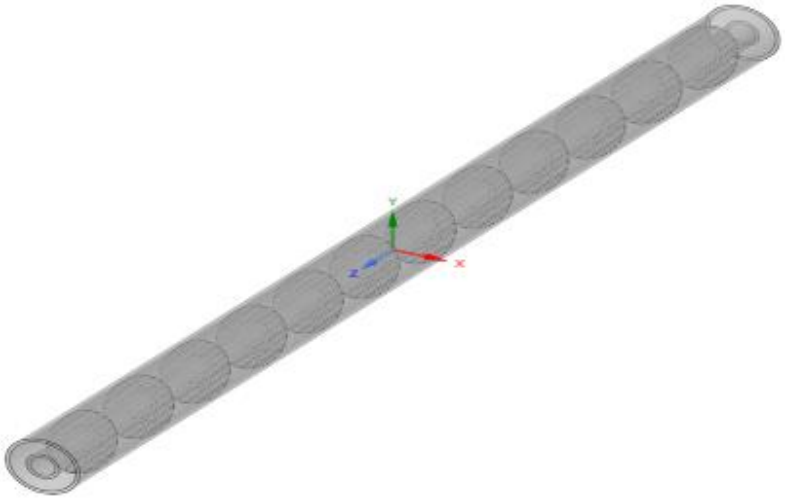

Figure 1. Isometric view

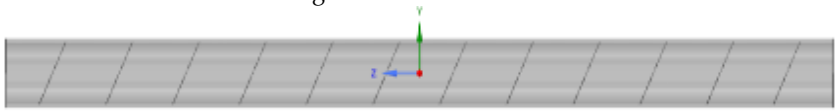

Figure 2. Side view

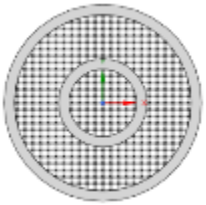

Figure 3. Front view

2.4 Mesh Independence Test

The mesh independence test is a standard numerical technique used to ensure that simulation results are not influenced by the discretization size. This verification step is critical, as overly coarse meshes can lead to inaccurate predictions, while unnecessarily fine meshes increase computational cost without significant gain in accuracy [17]. In this study, 26 mesh variations were evaluated by adjusting the element size from 0.13138 mm to 2.4 mm. Pressure drop was selected as the reference parameter for assessment. The simulation was repeated for each mesh configuration, and the percentage difference between successive results was calculated. Mesh independence was considered achieved when changes in pressure drop values between refinements fell below 1–5%, indicating numerical consistency and stability.

2.5 Model Validation

Model validation is the process of ensuring that the methods and computational instruments used in the study are sufficiently accurate and reliable to produce valid results. In this study, validation was carried out by comparing numerical simulation outputs with empirical calculations based on established correlations from previous research. The parameters used for validation are the Nusselt number (*Nu*). The Nusselt number used in the numerical simulation are calculated using Equations (1):

$$Nu = \frac{h.Dh}{k} \quad (1)$$

Where:
Nu : Nusselt number (dimensionless)
h : convective heat transfer coefficient (W/m²·°C)
Dh : hydraulic diameter of the pipe (m)
K : thermal conductivity of the fluid (W/m·°C)

For comparison and validation, the empirical correlations were used. The Nusselt number was validated against the Sieder–Tate correlation, as shown in Equations (2):

$$Nu = 0.027.Re^{0.8}.Pr^{\frac{1}{3}}.(\frac{di}{L})^{1/3}.(\frac{\mu\rho}{\mu\rho\omega})^{0.14} \quad (2)$$

Where:
Re : Reynolds number (dimensionless)
Pr : Prandtl number (dimensionless)
μp : dynamic viscosity of bulk fluid (kg/m·s)
μpw : dynamic viscosity at the wall temperature (kg/m·s)
di : inner diameter (m)
L : total pipe length (m)

These equations provide the theoretical benchmarks for validating the accuracy of the simulation results. Comparison between simulated and empirical values ensures the reliability of the CFD model used in this study. To ensure accurate prediction of turbulent flow behavior, especially near-wall treatment and flow separation induced by the wire mesh inserts, the SST k-ω turbulence model was adopted in ANSYS Fluent. This model combines the advantages of the k-ε model in the free stream and the k-ω model near walls, making it suitable for capturing the complex flow structures present in this study.

2.6 Data Analysis Method

This study employed a three-way Analysis of Variance to examine the influence of three independent variables which include wire mesh angle, wire spacing, and axial mesh spacing. The analysis focused exclusively on the Nusselt number as an indicator of heat transfer performance in the double pipe heat exchanger.

After determining the presence of significant effects, Tukey's Honestly Significant Difference test was used to identify statistically meaningful differences between factor levels and to determine the optimal configuration. Descriptive statistics were also calculated such as the mean, standard deviation, minimum, and maximum values for each experimental combination.

All statistical analyses, including three-way ANOVA and post hoc Tukey HSD tests, were performed using IBM SPSS Statistics Version 24 to ensure standardized and reproducible results.

The simulation results were organized into tables and figures. Contour plots of temperature fields were generated using ANSYS Fluent to enhance the understanding of thermal behavior under various configurations.

3. RESULTS AND DISCUSSION

3.1 Mesh Independency

The mesh independence test demonstrated clear stabilization of the pressure drop at mesh variation 19, with a minimum element size of 0.13145 mm and maximum of 1.4145 mm. As shown in Figure 4, the pressure drop recorded was 0.5963 Pa, which represents a convergent trend. Compared to the 18th variation (0.59707 Pa), the relative difference was 0.1288%, and only 0.014% when compared to the 20th variation (0.59622 Pa). These differences, being less than 0.1%, confirm that mesh independence was achieved and that further refinement has negligible influence on the simulation outcome.

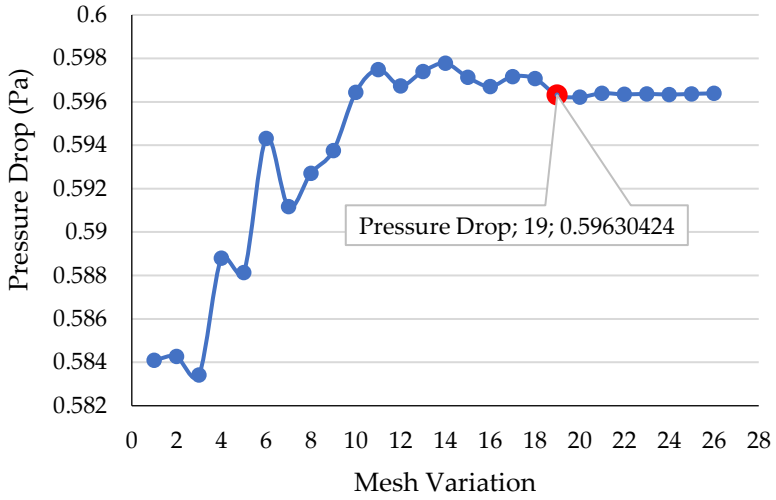

Figure 4. Pressure drop behavior in mesh independency

The observed stability in pressure drop indicates that the selected mesh configuration sufficiently resolves the flow dynamics. Early fluctuations in coarse meshes suggest inadequate representation of fluid-wall interactions. As the mesh becomes finer, geometric and viscous effects are captured more accurately, leading to convergence. This behavior is consistent with the theoretical basis of CFD, which relies on the conservation of mass and momentum. Finer meshes enhance the numerical accuracy of the Navier-Stokes equations [18].

Using finer meshes beyond this point would significantly increase computational cost without proportional gains in accuracy, consistent with the principle of diminishing returns [19]. Therefore, the 19th mesh variation is considered optimal, providing a balance between numerical accuracy and computational efficiency. All subsequent simulations on heat transfer analysis were performed using this mesh configuration to ensure high result validity.

3.2 Validation of the Numerical Model

Following the mesh independence test, model validation was performed to assess the accuracy of the plain tube simulation by comparing the predicted Nusselt number with the empirical Sieder-Tate correlation.

Figure 5 presents the comparison across Reynolds numbers, showing that the simulated Nusselt numbers were consistently lower than the correlation values. At Re = 4061, for instance, the simulation produced Nu = 14.06 compared to 15.64 from the correlation, with an average error of 18.34% over the full range. Despite this deviation, the increasing trend of the Nusselt number with Reynolds number is well captured.

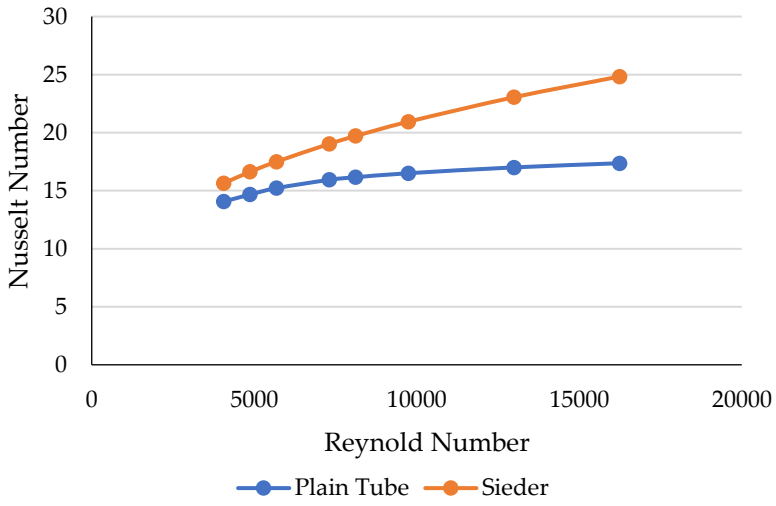

Figure 5. Comparison of simulated Nusselt number for plain tube with Sieder-Tate correlation

The discrepancy arises from the ideal assumptions in empirical correlations, such as constant fluid properties and fully developed thermal flow [20]. In contrast, numerical simulations account for mesh resolution, turbulence modeling, and thermophysical property variations, often yielding slightly conservative results [21][22].

The trend agreement and acceptable error margin confirm that the simulation model provides sufficiently accurate predictions of heat transfer, validating its use for further analysis [23][24].

Although the validation results fall within an acceptable error margin, the observed average deviation of approximately 18% from the Sieder–Tate correlation warrants further consideration. This discrepancy, while expected due to differences in modeling assumptions and empirical conditions, may introduce a degree of uncertainty in the absolute accuracy of the predicted Nusselt numbers. Nevertheless, the consistency of the trend and the relative performance across different configurations remain reliable, thereby preserving the integrity of the comparative analysis and the study's main conclusions.

3.3 Effect of Wire Mesh Variation on Heat Transfer

This section discusses the variation in Nusselt number as an indicator of convective heat transfer efficiency due to geometric modifications involving wire mesh inserts. The three main parameters varied in this study are mesh inclination angle, wire spacing, and axial mesh spacing.

Each parameter is expected to influence flow behavior and heat transfer mechanisms through turbulence enhancement and alteration of thermal boundary layers. The analysis presents the relationship between these geometrical factors and Nusselt number values to provide insight into how wire mesh configurations can be optimized to improve heat transfer performance in thermal engineering applications.

3.3.1 Simulated Nusselt Number Results

Nusselt numbers were obtained through heat transfer simulations using the Computational Fluid Dynamics (CFD) method in ANSYS Fluent. The simulations were conducted on a double pipe heat exchanger equipped with wire mesh inserts acting as turbulators. Data were collected at a Reynolds number of 4061 for the inner tube and 2070 for the outer tube. The Nusselt number values for each design variation are summarized in Table 3.

Table 3. Simulated Nusselt number for each configuration

Configuration	Nusselt Number
1	18.96187294
2	17.01152723
3	15.95506034
4	17.78884694
5	15.78787243
6	16.01578448
7	14.7760896
8	14.7929282
9	14.03927261

3.3.2 Normality, Homogeneity, and Three-Way ANOVA on Nusselt Number

To ensure the statistical validity of the ANOVA analysis, normality and homogeneity tests were performed on the Nusselt number data obtained from various wire mesh configurations. Normality was assessed using the Shapiro-Wilk method. As shown in Table 4, all groups based on wire mesh angle (30°, 60°, 90°), wire spacing (3 mm, 4 mm, 5 mm), and axial mesh spacing (4 cm, 5 cm, 6 cm) yielded significance values above 0.05. These results indicate that the Nusselt number data follow a normal distribution, satisfying a key assumption for ANOVA.

Table 4. Normality Test for Nusselt Number

Wire mesh angle		Kolmogorov-Smirnov[a]			Shapiro-Wilk		
		Statistic	df	Sig.	Statistic	df	Sig.
Nusselt Number	30°	0,244	3		0,971	3	0,675
	60°	0,223	3	.200*	0,909	3	0,429
	90°	0,265	3		0,864	3	0,274
Wire spacing							
Nusselt Number	3 mm	0,278	3		0,940	3	0,525
	4 mm	0,180	3	.200*	0,897	3	0,358
	5 mm	0,332	3		0,781	3	0,072
Axial mesh spacing							
Nusselt Number	4 cm	0,181	3		0,985	3	0,932
	5 cm	0,164	3	.200*	0,963	3	0,840
	6 cm	0,337	3		0,854	3	0,251

Levene's test was conducted to assess homogeneity of variances. As shown in Table 5, the significance values were 0.095 (mesh angle), 0.166 (wire spacing), and 0.338 (mesh spacing), all above the 0.05 threshold. This confirms the assumption of equal variances across groups, validating the use of ANOVA.

Table 5. Homogeneity of Variance for Nusselt Number

Factor	Levene Statistic	df1	df2	Sig.
Wire mesh angle	3.000	2	6	0.095
Wire spacing	2.165	2	6	0.166
Axial mesh spacing	1.213	2	6	0.338

Three-way ANOVA results in Table 6 demonstrate that all three independent variables had statistically significant effects on the Nusselt number, with p-values below 0.05. The mesh angle had the strongest effect ($F = 154.6$, $p < 0.001$), followed by wire spacing ($F = 63.69$, $p < 0.001$) and axial mesh spacing ($F = 22.98$, $p = 0.002$).

Table 6. Homogeneity of Variance for Nusselt Number

Source	DF	Adj SS	Adj MS	F-Value	P-Value
Wire mesh angle	2	14.6923	7.34617	154.6	0.000
Wire spacing	2	6.0531	3.02656	63.69	0.000
Axial mesh spacing	2	2.1836	1.0918	22.98	0.002
Error	2	0.2851	0.04752	–	–
Total	8	23.3912	–	–	–
R-sq = 98.78%. R-sq (adj) = 97.56%. R-sq (pred) = 92.88%					

The model explains 98.78% of the total variance (R^2), with adjusted R^2 of 97.56% and predicted R^2 of 92.88%, indicating strong model reliability. These results confirm that each geometric parameter significantly influences the convective heat transfer performance of the double pipe heat exchanger equipped with wire mesh inserts.

3.3.3 Post Hoc Analysis of Nusselt Number

Following the ANOVA results that confirmed all three geometric parameters significantly affect the Nusselt number, Tukey's Honestly Significant Difference (HSD) test was conducted to determine which levels within each factor contribute most to the differences observed.

As shown in Table 7, the 30° wire mesh angle produced the highest average Nusselt number (17.31), indicating optimal heat transfer performance. In contrast, 90° yielded the lowest value (14.52). A decreasing trend in performance with increasing angle suggests that smaller angles generate stronger flow disruption and promote local turbulence, thereby enhancing convective heat transfer [25].

Table 7. Mean Nusselt Number and Grouping Results for Each Geometric Parameter Based on Tukey HSD Test

Factor	Level	N	Mean	Grouping
Wire mesh angle	30°	3	17.31	A
	60°	3	16.41	B
	90°	3	14.52	C
Wire spacing	3 mm	3	17.17	A
	4 mm	3	15.89	B
	5 mm	3	15.40	C
Axial mesh spacing	4 cm	3	16.69	A
	5 cm	3	15.86	B
	6 cm	3	15.50	C

For wire spacing, 3 mm produced the highest mean value (17.17), followed by 4 mm (15.89) and 5 mm (15.40). Narrower spacing increases the number of obstacles per unit length, intensifying flow disturbances and promoting boundary layer disruption and thermal mixing [26][27]. Similarly, axial mesh spacing of 4 cm resulted in the best performance (16.69), with larger spacings showing reduced heat transfer due to weaker hydrodynamic interactions [28].

Table 8 presents the Tukey HSD results, which confirm that all level pairs with the greatest differences are statistically significant. For example, the 90°–30° comparison shows a mean difference of –2.757 ($p = 0.000$), while 60°–30° remains significant with a smaller but meaningful gap (–0.803, $p = 0.005$).

Table 8. Tukey HSD Pairwise Comparisons of Nusselt Number Differences Between Parameter Levels

Factor	Level Comparison	Difference of Means	SE	95% CI	T-Value	P-Value (Adjusted)
Wire mesh angle	60° – 30°	-0.803	0.158	(-1.288; -0.318)	-5.08	0.005
	90° – 30°	-2.757	0.169	(-3.275; -2.239)	-16.33	0.000
	90° – 60°	-1.954	0.142	(-2.390; -1.518)	-13.75	0.000
Wire spacing	4 mm – 3 mm	-1.265	0.158	(-1.750; -0.781)	-8.01	0.001
	5 mm – 3 mm	-1.893	0.169	(-2.411; -1.375)	-11.21	0.000
	5 mm – 4 mm	-0.628	0.142	(-1.064; -0.191)	-4.42	0.011
Axial mesh spacing	5 cm – 4 cm	-0.437	0.142	(-0.873; -0.001)	-3.08	0.049
	6 cm – 4 cm	-1.143	0.169	(-1.662; -0.625)	-6.77	0.001
	6 cm – 5 cm	-0.706	0.158	(-1.191; -0.221)	-4.47	0.010

Significant differences were also found between 3 mm and 5 mm wire spacing (–1.893, $p = 0.000$), and between 6 cm and 4 cm axial spacing (–1.143, $p = 0.001$), reinforcing that denser and more frequent flow obstruction enhances heat transfer. Excessive spacing weakens vortex formation and reduces thermal performance [29].

In summary, the 30° angle, 3 mm wire spacing, and 4 cm axial spacing consistently produced the highest thermal performance and belonged to Group A in Tukey's grouping. These findings align with forced convection theory, where geometric-induced flow disturbances improve the heat transfer coefficient and Nusselt number [30].

3.3.4 Effect of Wire Mesh Inclination Angle on Heat Transfer

Table 9 presents the Nusselt number statistics for three wire mesh inclination angles 30°, 60°, and 90°. For each angle, the mean, standard deviation, minimum, and maximum values are reported. The 30° configuration yielded the highest mean Nusselt number of 17.31, with a standard deviation of 1.52, a minimum of 15.95, and a maximum of 18.96. At 60°, the mean decreased to 16.41 (SD 0.83), with values ranging from 15.59 to 17.78. The 90° configuration showed the lowest mean of 14.52, with minimal variation (SD 0.35), ranging from 14.04 to 14.79.

Table 9. Nusselt Number by Wire Mesh Inclination Angle

Angle	Mean	SD	Min	Max
30°	17.31	1.52	15.95	18.96
60°	16.41	0.83	15.59	17.78
90°	14.52	0.35	14.04	14.79

A consistent trend is observed where smaller inclination angles result in higher convective heat transfer. A 30° mesh angle enhances surface interaction with the flow, intensifying turbulence and boundary layer disruption. This improves convective mixing and increases the heat transfer rate [31][32]. The wider Nusselt range at 30° also reflects complex yet effective flow dynamics. Statistical analysis via Tukey's test confirms that each angle level differs significantly, establishing 30° as the most effective configuration.

3.3.5 Effect of Wire Spacing on Heat Transfer

Table 10 presents Nusselt number values for different wire spacings of 3 mm, 4 mm, and 5 mm. The 3 mm configuration yielded the highest mean Nusselt number of 17.17 (SD 2.16), with a minimum of 14.77 and a maximum of 18.96. At 4 mm, the mean decreased to 15.89 (SD 1.08), and at 5 mm, it dropped further to 15.40 (SD 0.92).

Table 10. Nusselt Number Based on Wire Spacing

Wire Spacing	Mean	SD	Min	Max
3 mm	17.17	2.16	14.77	18.96
4 mm	15.89	1.08	14.47	17.01
5 mm	15.40	0.92	14.04	16.01

The data indicate that narrower wire spacing enhances convective heat transfer. The 3 mm configuration increases the number of flow disruptions per unit length, promoting frequent fluid–solid interactions, which intensify boundary layer disturbance and micro-vortex formation. These effects accelerate mixing and increase the local thermal gradient [33][34]. Although this configuration shows greater data variability, the dynamic flow contributes positively to convective enhancement. Considering mean values, standard deviations, and statistical significance confirmed by Tukey's test, the 3 mm spacing is identified as the most effective configuration for maximizing the Nusselt number.

3.3.6 Effect of Wire Mesh Spacing on Heat Transfer

Table 11 presents the Nusselt number for different axial spacings between wire mesh inserts 4 cm, 5 cm, and 6 cm. The 4 cm configuration yielded the highest average Nusselt number of 16.69 (SD 1.76), with a minimum of 14.79 and maximum of 18.96. At 5 cm spacing, the mean decreased to 15.86 (SD 1.45), while the 6 cm configuration showed the lowest average of 15.50 (SD 0.63), with a narrow range of 14.77–15.95.

Table 11. Nusselt Number Based on Wire Mesh Spacing

WM Spacing	Mean	SD	Min	Max
4 cm	16.69	1.76	14.79	18.96
5 cm	15.86	1.45	14.04	17.78
6 cm	15.50	0.63	14.77	15.95

The results indicate that larger spacing reduces heat transfer efficiency, as wider distances weaken the hydrodynamic interaction between successive mesh layers [35][36]. At 4 cm spacing, frequent flow disruptions enhance turbulence intensity and mixing zones, promoting thermal transport [37][38]. In contrast, 6 cm spacing allows flow re-stabilization before encountering the next mesh, limiting convective enhancement.

The higher standard deviation observed at 4 cm suggests more dynamic flow behavior, typical of transitional regimes that favor rapid boundary layer disruption and improved heat transfer [39]. Given its superior average performance, standard deviations, and wider range, the 4 cm spacing is identified as the most effective configuration. This conclusion is supported by Tukey's post hoc test, which confirmed statistically significant differences among all spacing levels.

While shorter axial mesh spacing (e.g., 4 cm) demonstrated improved heat transfer due to enhanced turbulence, it may also result in increased flow resistance and pressure drop. This trade-off is crucial in practical applications where pumping power and system efficiency must be balanced alongside thermal performance.

3.4 Comparison of Optimal Wire Mesh Design and Plain DPHE

A comparative analysis between the optimal wire mesh configuration and the plain double pipe heat exchanger (DPHE) shows consistent and significant improvement in convective heat transfer performance. Simulation results demonstrate an average increase of 34.55% in Nusselt number for the wire mesh configuration across Reynolds numbers from 4000 to 16000. This improvement corresponds to enhanced fluid–surface interaction and increased thermal mixing, which accelerate heat transfer [38]. The selected configuration with 30° angle, 3 mm wire spacing, and 4 cm axial spacing produces effective flow disruption without causing fluid stagnation. As shown in Figure 6, the Nusselt number for the wire mesh DPHE remains consistently higher than that of the plain system across all tested Reynolds numbers, indicating superior heat transfer performance.

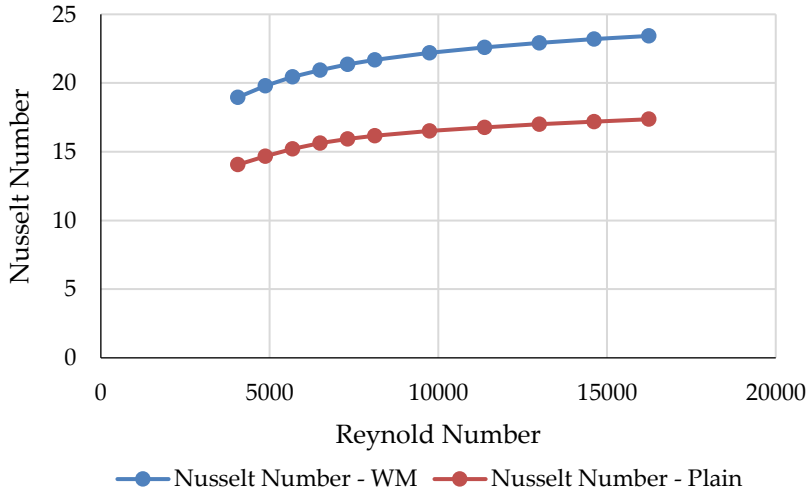

Figure 6. Nusselt number vs Reynolds number for optimal wire mesh design and plain DPHE configurations

From an industrial design perspective, while the optimal configuration of 30° angle, 3 mm wire spacing, and 4 cm axial spacing offers significant heat transfer enhancement, it may also lead to increased pressure drop and manufacturing complexity due to the tighter mesh structure. Therefore, real-world implementation would require balancing thermal performance gains against potential drawbacks such as higher pumping power and more intricate fabrication processes.

3.5 Temperature Contour Visualization of Optimal Wire Mesh vs Plain DPHE

Figures 7 illustrate temperature contours for two configurations of a double pipe heat exchanger (DPHE): (a) the optimal wire mesh design with 30° angle, 3 mm wire spacing, and 4 cm axial spacing, and

(b) the plain DPHE without mesh. Simulations were conducted at Reynolds numbers of 4061 (inner tube) and 2070 (outer tube).

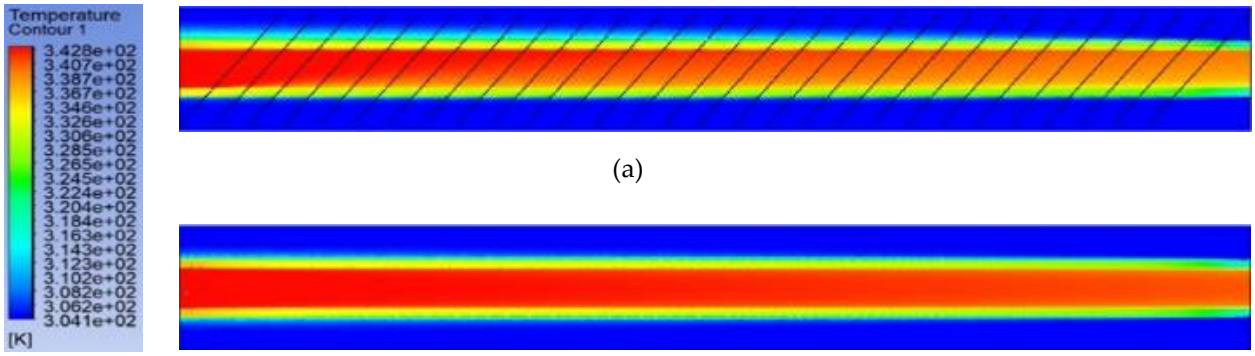

(a)

(b)

Figure 7. Temperature contours: (a) wire mesh DPHE shows enhanced thermal dispersion and stronger near-wall gradients; (b) plain DPHE shows more uniform core temperature with weaker boundary interaction

The wire mesh configuration shows sharper and more stratified thermal contours. Central regions with high temperature rapidly transition toward cooler zones near the wall, indicating strong temperature gradients. This pattern suggests enhanced mixing due to micro-vortices generated by the mesh, which accelerate convective heat transfer from the core to the wall [40][41].

The 30° mesh angle promotes stable crossflow without causing excessive frontal resistance. It supports longitudinal circulation and strengthens vortex structures [42]. The 3 mm wire spacing increases flow–surface interactions and reduces the thermal boundary layer [43][44]. Additionally, 4 cm axial spacing maintains turbulence while avoiding excessive pressure loss.

In contrast, the plain DPHE exhibits a nearly uniform high-temperature core with gradual cooling, indicating minimal mixing and thicker thermal boundary layers. Heat transfer relies more on conduction and the laminar bulk flow, resulting in a lower temperature drop and reduced Nusselt number, as also shown in earlier findings [45][46].

4. CONCLUSION

This study concludes that all wire mesh geometric parameters, including inclination angle, wire spacing, and axial spacing, significantly influence the heat transfer performance of the double pipe heat exchanger. The results of three-way ANOVA show strong statistical significance with p-values of 0.000 for wire mesh angle and wire spacing, and 0.002 for axial spacing. The highest F-value was observed for the wire mesh angle (154.6), followed by wire spacing (63.69) and axial spacing (22.98), indicating that wire mesh angle is the most dominant factor affecting the Nusselt number. The best thermal performance was achieved with a wire mesh angle of 30°, wire spacing of 3 mm, and axial spacing of 4 cm. These configurations yielded the highest average Nusselt numbers of 17.31, 17.17, and 16.69 respectively, and were consistently placed in the highest thermal performance group according to the Tukey HSD test. The 30° angle promoted intense flow disruption and enhanced turbulence near the thermal boundary layer. The 3 mm wire spacing increased vortex generation and fluid–solid interaction, while the 4 cm axial spacing maintained sustained turbulence without excessive flow resistance. This optimal configuration reached a maximum Nusselt number of 18.96, which was approximately 34.55% higher than the plain heat exchanger. Temperature contour visualizations supported these findings by revealing higher turbulence intensity and steeper thermal gradients along the pipe, confirming the effectiveness of wire mesh as a passive enhancement method for convective heat transfer. Future work may involve experimental validation of the numerical results and detailed analysis of pressure drop characteristics to better assess the practical feasibility of the proposed wire mesh configurations in industrial applications.

REFERENCES

[1] H. N. Sari, I. Made Arsana, and M. Hidayatulloh, "Pengaruh Fouling Factor Terhadap Performa Heat Exchanger Tipe Shell and Tube," vol. 8, no. 1, 2022.

[2] S. K. Singh, M. K. Chauhan, and A. K. Shukla, "Heat transfer enhancement in double-pipe heat exchanger: A review," in *Journal of Physics: Conference Series*, IOP Publishing Ltd, Feb. 2022. doi: 10.1088/1742-6596/2178/1/012007.

[3] A. Wahyuningsi *et al.*, "Installation Of Asbestos Insulation On Heat Exchangers Shell And Tube," 2022.

[4] A. Naufal, A. Ghifary, A. N. Hasya, T. Riadz, and L. Cundari, "Performance evaluation of heat exchanger on PE3 unit of PT. Lotte Chemical Titan Nusantara," 2022.

[5] S. Theeyzen and B. Freegah, "The effect of added wire mesh on the thermal efficiency of the flat plate solar water heater collector," *Results in Engineering*, vol. 24, Dec. 2024, doi: 10.1016/j.rineng.2024.103203.

[6] P. Raval, B. Ramani, N. J. Chotai, and K. Motwani, "Wire mesh-based heat transfer enhancement in absorber tube of solar collector-An experimental study," *International Journal of Thermofluids*, vol. 24, Nov. 2024, doi: 10.1016/j.ijft.2024.100878.

[7] K. BZare, D. Kanchan, and N. Patel, "Design Of Double Pipe Heat Exchanger."

[8] C. Ezgi and Ö. Akyol, "Thermal design of double pipe heat exchanger used as an oil cooler in ships: A comparative case study," *Journal of Ship Production and Design*, vol. 35, no. 1, pp. 12–18, Feb. 2019, doi: 10.5957/JSPD.170009.

[9] D. Ivananda, R. D. Ahmad, and M. A. I. Iswara, "Analisis Koefisien Perpindahan Panas Alat Double Pipe Heat Exchanger Berbasis Computational Fluid Dynamics," *DISTILAT: Jurnal Teknologi Separasi*, vol. 9, no. 3, pp. 240–250, Sep. 2023, doi: 10.33795/distilat.v9i3.3758.

[10] M. A. Sayed, A. M. T. A. ELdein Hussin, N. A. Mahmoud, and W. Aboelsoud, "Performance evaluation of wire mesh heat exchangers," *Appl Therm Eng*, vol. 169, Mar. 2020, doi: 10.1016/j.applthermaleng.2019.114891.

[11] S. Lal, V. Fuskele, and R. M. Sarviya, "Effect Of Wire Mesh Insert On Heat Transfer And Pressure Drop In Double Pipe Heat Exchanger," 2019. [Online]. Available: https://www.researchgate.net/publication/342000583

[12] R. Kurian, C. Balaji, and S. Venkateshan, "Experimental investigation of near compact wire mesh heat exchangers," *Appl Therm Eng*, 2016, doi: 10.1016/j.applthermaleng.

[13] E. Usama, N. Abd El Aziz, W. Aboelsoud, and A. Mohammed, "Numerical Investigation Of Heat Transfer And Pressure Drop Of Cross-Flow Woven Wire Mesh Heat Exchanger."

[14] D. Gaikwad and K. Mali, "Heat Transfer Enhancement for Double Pipe Heat Exchanger Using Twisted Wire Brush Inserts," 2014. [Online]. Available: www.ijirset.com

[15] K. Sharifi, M. Sabeti, M. Rafiei, A. H. Mohammadi, and L. Shirazi, "Computational fluid dynamics (CFD) technique to study the effects of helical wire inserts on heat transfer and pressure drop in a double pipe heat exchanger," *Appl Therm Eng*, vol. 128, pp. 898–910, 2018, doi: 10.1016/j.applthermaleng.2017.08.146.

[16] S. Kotian, N. Methekar, N. Jain, and P. Naik, "Asian Review of Mechanical Engineering Heat Transfer and Fluid Flow in a Double Pipe Heat Exchanger, Part I: Experimental Investigation," vol. 9, no. 2, pp. 7–15, 2020.

[17] B. Lopes, M. R. T. Arruda, L. Almeida-Fernandes, L. Castro, N. Silvestre, and J. R. Correia, "Assessment of mesh dependency in the numerical simulation of compact tension tests for orthotropic materials," *Composites Part C: Open Access*, vol. 1, Aug. 2020, doi: 10.1016/j.jcomc.2020.100006.

[18] G. Sun, J. A. Domaradzki, X. Xiang, and K. K. Chen, "Assessing accuracy of CFD simulations through quantification of a numerical dissipation rate," 2017.

[19] A. Lv, G. Ding, and X. Luo, "Influence of elevation angle of tundish filter on removal rate of impurity in molten steel," *Sci Rep*, vol. 15, no. 1, Dec. 2025, doi: 10.1038/s41598-024-84999-5.

[20] B. Güler, "Comparative Analysis of Heat Transfer Coefficient Using Experimental Data and Empirical Expressions."

[21] K. Kim, J. P. Hickey, and C. Scalo, "Pseudophase change effects in turbulent channel flow under transcritical temperature conditions," *J Fluid Mech*, vol. 871, pp. 52–91, Jul. 2019, doi: 10.1017/jfm.2019.292.

[22] G. Araya, "Turbulence model assessment in compressible flows around complex geometries with unstructured grids," *Fluids*, vol. 4, no. 2, Jun. 2019, doi: 10.3390/fluids4020081.

[23] W. Febrian, M. Anggara, and F. Dzil Ikram, "Analisis Distribusi Panas pada Variasi Posisi Pipa dan Diameter Pipa Penghantar Panas terhadap Efesiensi Pengeringan Rengginang Menggunakan Computational Fluid Dynamic (CFD)," vol. 14, no. 2, pp. 36–49, 2023.

[24] N. Ikhwan, "Validasi Pemodelan Heat Exchanger Dalam Computational Fluid Dynamics (CFD)," 2010.

[25] N. Ali *et al.*, "Numerical investigation on heat transfer and flow mechanism in microchannel heat sink having V shape ribs," *Case Studies in Thermal Engineering*, vol. 65, Jan. 2025, doi: 10.1016/j.csite.2024.105684.

[26] T. R. Chiaradia, G. F. M. de Carvalho, A. M. Bimbato, and L. A. Alcântara Pereira, "A Contribution to the Temperature Particles Method—Implementation of a Large-Eddy Simulation (LES) Model for the Temperature Field," *Applied Sciences (Switzerland)*, vol. 15, no. 8, Apr. 2025, doi: 10.3390/app15084122.

[27] W. Hu, S. Hickel, and B. W. Van Oudheusden, "Low-frequency unsteadiness mechanisms in shock wave/turbulent boundary layer interactions over a backward-facing step," *J Fluid Mech*, vol. 915, 2021, doi: 10.1017/jfm.2021.95.
[28] O. Volodin, N. Pecherkin, and A. Pavlenko, "Combining Microstructured Surface and Mesh Covering for Heat Transfer Enhancement in Falling Films of Refrigerant Mixture," *Energies (Basel)*, vol. 16, no. 2, Jan. 2023, doi: 10.3390/en16020782.
[29] H. A. Abotaleb, M. Y. Abdelsalam, and M. M. Aboelnasr, "Effect of wire mesh on the heat transfer from a flat plate under free water jet impingement quenching," *Alexandria Engineering Journal*, vol. 57, no. 4, pp. 3841–3850, Dec. 2018, doi: 10.1016/j.aej.2018.02.005.
[30] G. A. Q. Abdulrahman and M. Alharbi, "Laminar and turbulence forced heat transfer convection correlations inside tubes. A review."
[31] Y. H. Assaf, A. Akroot, K. Alnamasi, and M. A. Ismail, "Investigation of heat transfer performance in heat exchangers using hybrid nanofluids and twisted tape inserts with fixed special rings," *Sci Rep*, vol. 15, no. 1, Dec. 2025, doi: 10.1038/s41598-025-02135-3.
[32] F. E. Ames, "Turbulence Effects on Convective Heat Transfer," in *Handbook of Thermal Science and Engineering*, Springer International Publishing, 2017, pp. 1–33. doi: 10.1007/978-3-319-32003-8_17-1.
[33] S. Eiamsa-Ard, N. Koolnapadol, and P. Promvonge, "Heat transfer behavior in a square duct with tandem wire coil element insert," *Chin J Chem Eng*, vol. 20, no. 5, pp. 863–869, 2012, doi: 10.1016/S1004-9541(12)60411-X.
[34] R. Rezaey, "Experimental Investigation of Heat Transfer in Laser Sintered and Wire Mesh Heat Exchangers," 2017.
[35] A. Martín Subirana, J. P. Solano, R. Herrero-Martín, A. García, and J. Pérez-García, "Mixed convection phenomena in tubes with wire coil inserts," *Thermal Science and Engineering Progress*, vol. 42, Jul. 2023, doi: 10.1016/j.tsep.2023.101839.
[36] J. Long, B. W. Yang, T. Wu, and B. Zhang, "Numerical investigation of turbulent mixed convection flow and heat transfer characteristics of 2 × 2 subchannels with spacer grids," *Energy Sci Eng*, vol. 11, no. 3, pp. 1005–1024, Mar. 2023, doi: 10.1002/ese3.1386.
[37] P. Phani Kumar, A. C. Mandal, and J. Dey, "Effect of a mesh on boundary layer transitions induced by free-stream turbulence and an isolated roughness element," *J Fluid Mech*, vol. 772, pp. 445–477, Jun. 2015, doi: 10.1017/jfm.2015.203.
[38] J. H. Harmening, H. Devananthan, F. J. Peitzmann, and B. O. el Moctar, "Aerodynamic Effects of Knitted Wire Meshes—CFD Simulations of the Flow Field and Influence on the Flow Separation of a Backward-Facing Ramp," *Fluids*, vol. 7, no. 12, Dec. 2022, doi: 10.3390/fluids7120370.
[39] R. D. Selvakumar and H. Lee, "Thermal boundary layer depletion in minichannels by electrohydrodynamic conduction pumping," *Appl Therm Eng*, vol. 230, Jul. 2023, doi: 10.1016/j.applthermaleng.2023.120758.
[40] G. Hu, Z. Wang, Q. Gao, Q. Yang, and F. Peng, "Study on heat transfer in self-excited oscillation with backflow vortex disturbance effect," *J Thermophys Heat Trans*, vol. 35, no. 3, pp. 569–579, 2021, doi: 10.2514/1.T6172.
[41] R. Nanda Parely and A. Firdaus Sudarma, "Pengaruh Guide Vanes Terhadap Aliran Udara Pada Saluran Dengan Variasi Kecepatan Aliran Menggunakan Ansys Fluent," *Jurnal Sain dan Teknik*, vol. 5, no. 1, 2023.
[42] K. Blanckaert and H. J. de Vriend, "Secondary flow in sharp open-channel bends," *J Fluid Mech*, vol. 498, pp. 353–380, Jan. 2004, doi: 10.1017/S0022112003006979.
[43] M. E. Siddiqui, A. A. Melaibari, and F. S. Butt, "Experimental Investigation of Temperature Distribution in a Laminar Boundary Layer over a Heated Flat Plate with Localized Transverse Cold Air Injections," *Energies (Basel)*, vol. 16, no. 17, Sep. 2023, doi: 10.3390/en16176171.
[44] K. Zhu, W. D. Liu, and M. B. Sun, "Impacts of periodic disturbances on shock wave/turbulent boundary layer interaction," *Acta Astronaut*, vol. 182, pp. 230–239, May 2021, doi: 10.1016/j.actaastro.2021.02.017.
[45] A. Sukhanovskii and A. Evgrafova, "Dependence of boundary layer thickness on layer height for extended localised heaters," *Exp Therm Fluid Sci*, vol. 121, Feb. 2021, doi: 10.1016/j.expthermflusci.2020.110275.
[46] K. J. Hopkins, H. Porat, T. J. McIntyre, V. Wheatley, and A. Veeraragavan, "Measurements and analysis of hypersonic tripped boundary layer turbulence," *Exp Fluids*, vol. 62, no. 8, Aug. 2021, doi: 10.1007/s00348-021-03254-z.